

# Novel Intramolecular Hydrogen Abstraction Photosensitizers (IHA-PS) for Cationic UV Curable Systems

Zhigang Chen and Dean C. Webster\*

*Department of Coatings and Polymeric Materials  
Center for Nanoscale Science and Engineering  
North Dakota State University  
1735 NDSU Research Park Drive, Fargo, ND 58105*

## Abstract

Novel cationic Intramolecular Hydrogen Abstraction Photosensitizers (IHA-PS) were synthesized and found to have a pronounced photosensitization effect in cycloaliphatic epoxide based cationic UV curable systems using sulfonium salt photoinitiators. A series of polyol based photosensitizers were synthesized with naphthalene attached. One polyol photosensitizer, P-Na, was found to have a much pronounced photosensitization effect in three formulation systems different in crosslink density and mobility as revealed by real time FTIR (RTIR) experiments. Such phenomenon is explained by a proposed facile Intramolecular Hydrogen Abstraction Photosensitization (IHAP) mechanism, which is possible only with the unique molecular structure of P-Na. Two non-polyol type photosensitizers were also synthesized and compared with P-Na, the result further confirmed the more pronounced photosensitization effect of P-Na. To verify the proposed mechanism and obtain a more efficient IHA-PS, a “designed” IHA-PS molecule was synthesized utilizing proposed key principles in IHAP mechanism. The “designed” IHA-PS achieved similar photosensitization effect to P-Na with only half of its molecular weight and one third of its hydroxyl groups per molecule, which further validates the proposed photosensitization mechanism.

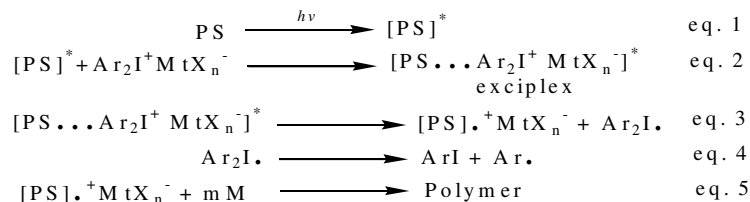
## 1. Introduction

Cationic UV curable systems have received considerable attention and are experiencing rapid development in recent years due to the advantages such as no oxygen inhibition, low energy requirement, a solvent free process and high polymerization rate.<sup>1,2</sup> Among the many monomer-photoinitiator combinations for cationic UV curable formulations, the combination of cycloaliphatic epoxide monomer and onium salt – especially sulfonium salt photoinitiators – have been widely adopted since it provides higher reactivity, higher thermal stability and good coating properties.<sup>1,3,4</sup> However, the curing speed and reactive functional group conversion for these cationic UV curable systems are still not as high as those with free radical systems.<sup>1</sup> One of the important reasons is that the onium salt photoinitiators have limited absorption in the long wavelength region of UV spectrum. Thus, much of the energy emitted by broadband light sources such as the commonly used mercury arc lamps is wasted.<sup>5</sup> To overcome this drawback, the addition of photosensitizers may be used to extend the sensitivity of the coating system at longer UV wavelengths.<sup>6-8</sup> Electron transfer photosensitization is considered the most efficient and

---

\* Corresponding author: Phone: (701) 231-8709. Fax: (701) 231-8439. E-mail: [dean.webster@ndsu.edu](mailto:dean.webster@ndsu.edu)

generally applicable process for onium salt photoinitiators, which is a photoinduced redox process in essence.<sup>5,9,10</sup> A generalized photosensitization mechanism for onium salts is shown in Scheme 1 using a diaryliodonium salt as an example. Similar mechanisms can be written for the photosensitization of other onium salt photoinitiators such as triarylsulfonium and dialkylphenacylsulfonium salts.



Scheme 1. Generalized photosensitization route for onium salt photoinitiators.<sup>5</sup>

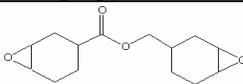
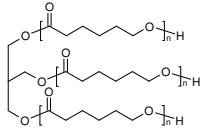
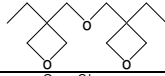
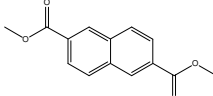
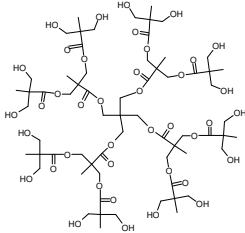
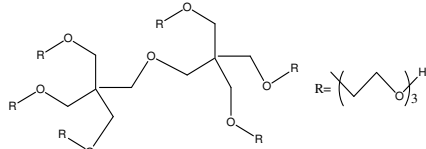
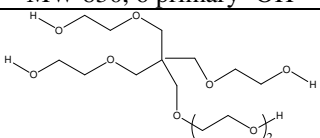
In Scheme 1, the photosensitizer (PS) is first excited to the excited state after the absorption of light (eq. 1); then, an excited state complex (exciplex) is formed as an intermediate between the onium salt and the excited photosensitizer (eq. 2). Subsequently, an electron is transferred from the PS to the photoinitiator, which induces its decomposition and yields a diaryliodonium free radical and the photosensitizer cation radical paired with the anion  $\text{MtX}_n^-$  (eq. 3). The rapid decomposition of the resulting unstable diaryliodonium free radical (eq. 4) prevents the back electron transfer and renders the overall process essentially irreversible. The cationic polymerization (eq. 5) takes place either by the direct interaction of the monomer with the photosensitizer cation radical or by first radical dimerization and then polymerization by the resulting dication. During electron transfer photosensitization, both the onium salt and the photosensitizer are irreversibly consumed.<sup>5, 11</sup>

Due to their higher reduction potential, sulfonium salt photoinitiators, unlike diaryliodonium salts, can only be effectively sensitized by electron rich polynuclear aromatic compounds such as anthracene, pyrene and perylene.<sup>10, 12-13</sup> Since the solubility of the photosensitizer is one of the key factors for effective photosensitization, polynuclear aromatic sensitizers are often chemically modified to have improved solubility and reduced toxicity.<sup>12</sup> Previous work in this lab has shown that by attaching naphthalene or anthracene moieties to formulation components such as oxetane and polyol, the solubility of these chromophores in the coating matrix were improved. As a result, the photosensitization effect of these photosensitizers was enhanced and more complete cure of the coatings was achieved.<sup>14</sup> It appears to be advantageous to attach polynuclear aromatic compounds to polyol species due to their good compatibility with most of the cationic UV curable formulation ingredients. In this contribution we report a group of novel polyol based cationic photosensitizers which have a pronounced photosensitization effect, and propose an Intramolecular Hydrogen Abstraction Photosensitization (IHAP) mechanism to account for the experimental observations. The photosensitizers that function through the proposed IHAP mechanism are called IHA-PS (Intramolecular Hydrogen Abstraction Photosensitizers) in this paper.

## 2. Experimental

**2.1. Materials used.** Chemicals used in the photosensitizer synthesis and coating formulations in this work are listed in Table 1. HPLC grade THF and acetone, triethylene amine (TEA), and Amberlyst® 15 - sulfonic acid functionalized ion exchange resin were obtained from Aldrich. All materials were used as received.

Table 1. Chemicals used in photosensitizer synthesis and coating formulation.

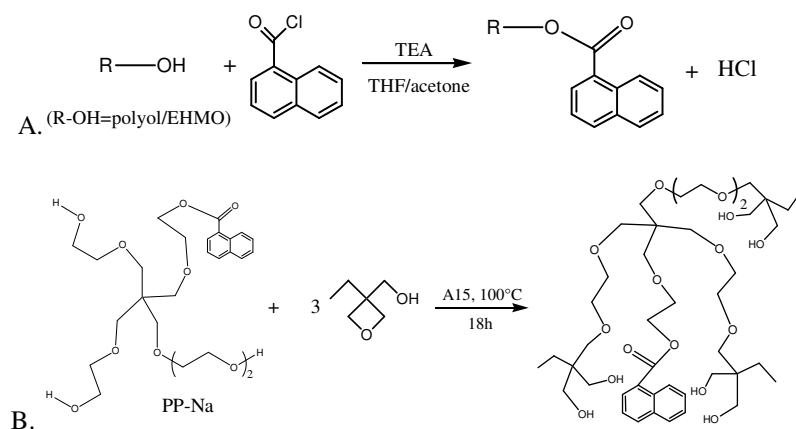
Name	Abbreviation	Source	Chemical Structure/description
UVI 6974	PI	Dow	mixed triarylsulfonium hexafluoroantimonate salt in propylene carbonate
UVR 6110	ECC	Dow	
UVR 6000	EHMO	Dow	
Tone 301	PCL	Dow	 MW 300, 3 primary hydroxyls
OXT-221	DOX	Toagosei Co. Ltd	
1-Naphthol chloride	1-Na Cl	Aldrich	
Dimethyl 2,6-naphthalene dicarboxylate	NDC	Aldrich	
P1000	P	Perstorp Polyols Inc.	 Second generation dendritic polyester polyol (shown above) blended with polyether polyol; MW 1500, 15 primary -OH
DPP130	DPP	Perstorp Polyols Inc.	 MW 830, 6 primary -OH
PP50s	PP	Perstorp Polyols Inc.	 MW 356, 4 primary -OH

## 2.2 Synthesis and characterization of photosensitizers.

A series of photosensitizers were synthesized in this work; structures and nomenclature are shown in Table 3. The synthesis of NDC-OX was described previously.<sup>14</sup> The synthesis of photosensitizers P-Na, PP-Na, DPP-Na, PCL-Na and OXT-Na are based on the reaction between hydroxyl groups and 1-naphthol chloride (1-Na Cl) as shown in Scheme 2A. The general procedure of the synthesis is as follows: the hydroxyl containing compound R-OH (polyol or EHMO) was dissolved

in ~5 g HPLC grade THF or acetone in a 20ml glass vial, then an equal molar amount of 1-Na Cl was added into the vial. The mixture was stirred using a magnetic stir bar for ~ 5 minutes in an ice-water bath, followed by the dropwise addition of TEA in twice the molar amount required to neutralize the HCl generated in the reaction. The white TEA-HCl salt soon precipitated. When the addition of TEA (~ 2 minutes) was completed, the mixture was stirred for another 10 minutes followed by the addition of 10 g THF or acetone. The mixture was then filtered twice to remove the TEA-HCl salt. The filtered solution was heated on a hotplate at about 100 °C under N<sub>2</sub> purge for ~ 1h, followed by vacuum (30mm Hg) at room temperature for 1h to remove residual solvent and TEA.

The synthesis route of photosensitizer PP-Na-ol is shown in Scheme 2B. The synthesis was carried out as follows: 1.02 g PP-Na, 0.696 g EHMO (mole ratio 1:3) and 0.09g A15 (~5 wt % of total resin) were mixed in a 20 ml glass vial, the mixture was heated at 100 °C with magnetic stirring for 16 h. Then 10 g mixed solvent of THF and acetone was added and the solution was filtered to remove the solid catalyst. The filtrate was then heated at 100 °C under N<sub>2</sub> purge for 1 h, followed by vacuum at ~ 65 °C for 3 h to remove the residual solvent.



Scheme 2. Synthesis routes for photosensitizer synthesis.

The synthesized photosensitizers were characterized by high performance liquid chromatography (HPLC) and GC-MS. The HPLC analysis was performed on an Agilent 1100 series HPLC utilizing the diode array detector (DAD) for UV-Vis characterization. Chromatographic separation was achieved on a reversed-phase ZORBAX C-18 column with a C4 guard column. The mobile phase consisted of two solvents: Solvent A (HPLC grade water) and solvent B (acetonitrile). Column temperature was maintained at 40 °C throughout the analysis. A 1 µl injection volume was used for all samples. The column was eluted with the following gradient: 0 min, 10% B; 30 min, 100% B; 40 min, 100% B; 40.1 min, 10% B. Flow rate was 1.5 ml/min with a 45 minute runtime per injection. The GC-MS analysis was performed on HP 6890 gas chromatograph and HP 5973 mass selective detector utilizing EI (electron ionization) with filament energy of 69.9 keV. The front inlet was in split mode with inlet temperature of 250 °C and pressure 8.24 psi.; split ratio was 50:1. Initial GC oven temperature was 70 °C for 2 minutes, then the temperature was ramped to 300 °C at a rate of 20 °C/min and was hold for 16.5 minutes. Total run time was 30 minutes. Separation was achieved on a ZEBRON ZB-35 capillary column operated in a constant flow mode with flow rate of 1.0ml/min., the average velocity is 36 cm/s. the mass spectrometer was in scan mode with m/z range from 10 to 800. The temperature for MS source and MS Quad were set at 230 °C and 150 °C respectively.

### 2.3. Sensitized coating formulation and characterization.

The synthesized photosensitizers were added into three different coating formulation systems to examine their photosensitization effect. In order to reduce variation, a master base for each system was made and named EHMO MB, DOX MB and PCL MB respectively. The compositions of these coating formulation systems are shown in Table 2. Because of the different reactive diluents, these three formulation systems have different crosslink density (XLD) and mobility. For the system ECC-DOX, its reactive monomers are all difunctional, as a result it has the highest XLD and earliest vitrification point among the three systems. While for system ECC-PCL, it has the lowest XLD and highest mobility due to the existence of PCL. As to system ECC-EHMO, its XLD and mobility are in between.<sup>14</sup>

Table 2. The compositions of three different coating formulation systems.

Formulation systems / Ingredients	ECC	PI	Reactive diluent
ECC-EHMO MB			EHMO 15 wt%
ECC-DOX MB	80 wt%	4 wt%	DOX 15 wt%
ECC-PCL MB			PCL 15 wt%

Sensitized coating formulations were made by adding  $1 \times 10^{-4}$  mole photosensitizer (theoretical MW of photosensitizers was used for calculation) to 5 g master base coating; this amounts to the addition of ~ 1-3 wt% photosensitizer. The mixture was then heated on hotplate for ~ 15 min. to dissolve the photosensitizer in the coating. Because of the different crosslink density and mobility of the three formulation systems, the same photosensitizer was expected to exhibit different photosensitization effect since the mobility of a coating system is closely related to the photosensitization ability of a photosensitizer.<sup>14,15</sup>

The UV curing behavior of the sensitized coatings was monitored in real time FTIR (RTIR) experiments. The real time FTIR experiments were performed using a Nicolet Magna-IR 850 spectrometer Series II with detector type DTGS KBr, with a UV optic fiber mounted in a sample chamber in which humidity was kept constant at around 20% by Drierite<sup>®</sup>. The light source was a LESCO Super Spot MK II 100W DC mercury vapor short-arc lamp. Coating samples were spin coated onto a KBr plate at 3000 rpm for about 15 s, which were then exposed to UV light for 60 s. Scans were taken over a 120 s period at 2 scan/s. The UV source was adjusted to  $\sim 3.6 \text{ mW/cm}^2$  and the experiments were performed in air. The oxirane conversion of ECC was monitored at  $789 \text{ cm}^{-1}$ , the oxetane conversion of EHMO and DOX was monitored at  $976\text{-}977 \text{ cm}^{-1}$ . The RTIR was considered as a more direct and sensitive monitoring technique since it specifically monitors the reaction of the photo reactive functional groups upon lower UV light intensity. The average standard deviation for the RTIR measurement is  $\pm 2\%$ . A typical reactive functional group conversion – time plot obtained in the RTIR experiment is shown in Figure 1.

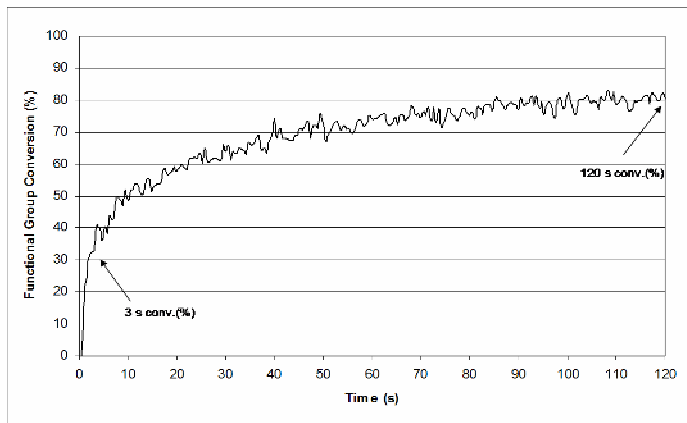


Figure 1. A typical reactive functional group conversion – time plot obtained in the RTIR experiment.

For the RTIR experiment results, the reactive functional group conversion after 3 s and 120 s reaction (abbreviated as 3 s conversion and 120 s conversion herein) are presented. It was reported that the photopolymerization will not be interfered by the vitrification at the initial stage, and the slope of the conversion versus time plot in the initial linear portion is directly proportional to the rates of photopolymerization.<sup>12</sup> From Figure 1 it can be seen that within 3 seconds the conversion versus time plot is still in the linear range, thus the 3 s conversion is used here as a simplified representation of the slope and the unperturbed photopolymerization rate. On the other hand, Figure 1 shows that the 120 s conversion data lies in the plateau portion of the conversion-time plot, thus it is used to represent the ultimate conversion of the photo reactive functional groups.

### 3. Results and Discussion

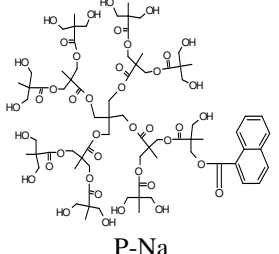
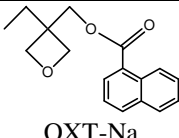
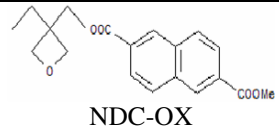
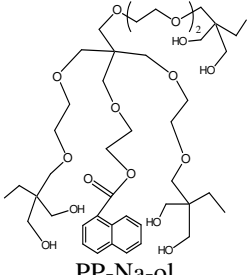
#### 3.1. Synthesis and characterization of photosensitizers.

The synthesis, characterization, purity and nominal structure of the photosensitizers synthesized in this work are summarized in Table 3. In Table 3, DPP-Na, PCL-Na and PP-Na all have similar nominal structure to that of P-Na but with different polyols attached to naphthalene. The formation of desired products was confirmed by HPLC and GC-MS, and the purity was obtained by the peak area integration from HPLC or GC-MS chromatograms of the synthesis products. Figure 2 shows the UV-Vis spectra of PP-Na-ol, 1-naphthalene carboxylic acid and EHMO respectively as obtained from the UV-Vis detector of the HPLC. Similar to the EHMO, all of the polyol reactants used in this work have no absorption above 250 nm in the UV-Vis spectrum as well.

#### 3.2. Photosensitizer performance in Cationic UV Curable Systems.

In the trial synthesis of new UV laser ablation sensitizers, a series of polyol based sensitizers (P-Na, DPP-Na and PCL-Na) were synthesized in order to improve the solubility of naphthalene in the coating matrix. These sensitizers were then added into three different coating formulation systems. These polyol based sensitizers were expected to have a similar photosensitization effect in the same coating system due to their good solubility and the same molar amount added. RTIR was then used to monitor the UV curing behavior of the sensitized coatings; the results are shown in Figure 3.

Table 3. Sensitizers synthesized in this work.

Photosensitizer synthesized	Reactant 1	Reactant 2	Product appearance	Synthesis route	Characterization and product purity
DPP-Na	DPP	1-Na Cl	pale yellow liquid	Scheme 2A	HPLC, 96.4%
PCL-Na	PCL				HPLC, 81.4%
PP-Na	PP				HPLC, 94.0%
 P-Na	P	EHMO		Scheme 2A	HPLC, 95.5%
 OXT-Na	EHMO				GC-MS, 100%
 NDC-OX	EHMO	NDC	white solid powder	Transesterification	GC-MS, 71.8%
 PP-Na-ol	PP-Na	EHMO	light brown liquid	Scheme 2B	HPLC, 95.7%

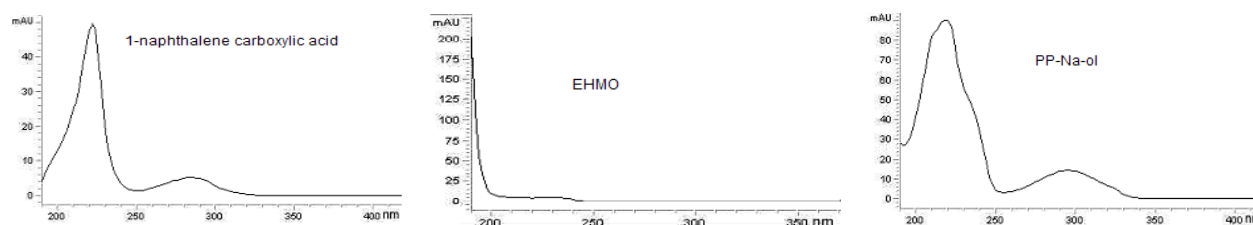


Figure 2. UV-Vis spectra of 1-naphthalene carboxylic acid, EHMO and PP-Na-ol.

In all of the coating formulation systems, the sensitized coatings exhibited higher initial photopolymerization rate and final conversion than the blank samples (master base formulations) as revealed by the RTIR 3 s and 120 s conversion data, which was expected. At the same time, it was noted that in the system ECC-EHMO and ECC-PCL, one particular photosensitizer, P-Na, exhibited a much more pronounced photosensitization effect than the other two polyol based photosensitizers – both the initial photopolymerization rate and the final functional group conversion are much higher. In system ECC-DOX, because of the lower system mobility and earlier vitrification point, the photosensitization effect is compromised thus not much difference is observed between the different formulations.

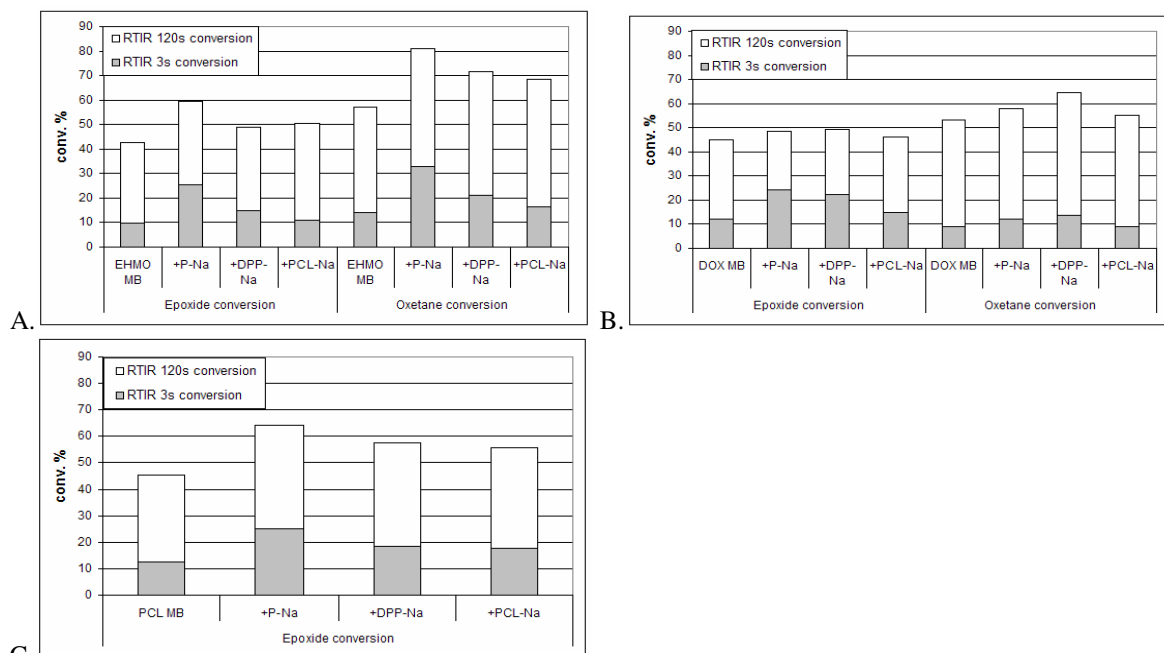


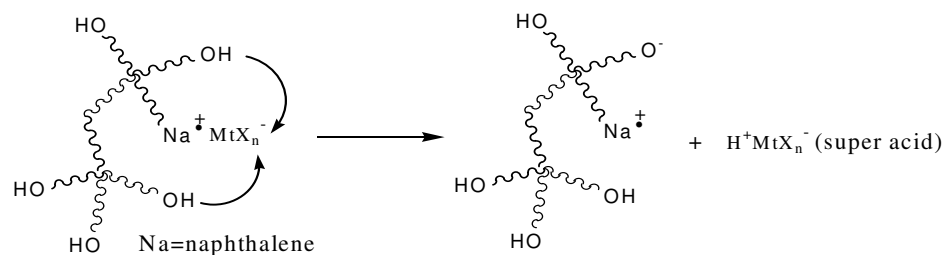
Figure 3. Functional group conversion of coatings sensitized by different polyol sensitizers in RTIR experiments. A) System ECC-EHMO. B) System ECC-DOX. C) System ECC-PCL.

### 3.3. Proposal of the Intramolecular Hydrogen Abstraction Photosensitization (IHAP) mechanism.

The better photosensitization effect of P-Na was considered, and the difference in the molecular structures of these polyol based photosensitizers was considered to be a major cause. Consequently, it was thought that the P-Na must possess some particular structural features that endow it with a more pronounced photosensitization effect. In the cationic UV photoinitiation process, after the photodecomposition of the photoinitiator, the released anion often abstracts a hydrogen from surrounding hydrogen donors (water in air, solvents and monomers in the coating system etc.) to generate a super acid  $H^+M_tX_n^-$  which then protonates the monomers to initiate polymerization.<sup>4</sup> When a photosensitizer exists in the system, the photoinitiation follows a different route as shown in eq. 3 Scheme 1. The excited photosensitizer first aids the decomposition of photoinitiator through an electron transfer mechanism. Then the anion species that is originally paired to the photoinitiator cation will be paired with the photosensitizer cation radical;<sup>5</sup> consequently, it is possible for this new ion pair to abstract a surrounding hydrogen to form a super acid species.

By understanding this photosensitization mechanism and the molecular structure of P-Na, we propose an *Intramolecular Hydrogen Abstraction Photosensitization (IHAP) mechanism* to explain the above experimental observations. The proposed mechanism is illustrated in Scheme 3 and is described as follows: In a P-Na aided photoinitiation process, a new ion pair  $Na^+MtX_n^-$  is formed first as shown in Scheme 3. This new ion pair is attached to one of the branch ends of a globular dendritic polyol molecule (polyol P) which has a large amount of hydroxyl groups on the surface (16 hydroxyls theoretically); the distance between any of the adjacent branches is therefore short. This relative spatial position of  $Na^+MtX_n^-$  and the dense surrounding hydroxyl groups provides a greater chance for  $Na^+MtX_n^-$  to interact and abstract a hydrogen intramolecularly from the polyol molecule to generate the super acid. Since an intramolecular process is much faster than an intermolecular one, the super acid generation rate is consequently faster. As a result, the whole photoinitiation process is faster which eventually induces a faster photopolymerization conversion. A photosensitizer that functions through the

proposed IHAP mechanism is called an Intramolecular Hydrogen Abstraction – Photosensitizer (IHA-PS).



Scheme 3. Illustration of super acid generation through Intramolecular Hydrogen Abstraction by  $\text{MtX}_n^-$ .

Compared to the P-Na, the IHAP mechanism has less of a chance to occur in the photosensitization process involving DPP-Na and PCL-Na considering their nominal molecular structures. For PCL-Na, only two internal hydroxyls are around the ion pair  $\text{Na}^+\text{MtX}_n^-$ . Moreover, the interaction of the ion pair and the hydroxyls relies on the movement of a relatively rigid ester bond and hydrocarbon chain. These factors result in a generally worse photosensitization effect of PCL-Na. As to DPP-Na, the distance between the ion pair and internal hydroxyls is actually longer than that in the PCL-Na molecule, but the flexibility of the ether linkage and higher hydroxyl content in the molecule seem to compensate for the distance disadvantage well, thus DPP-Na has a better photosensitization effect than PCL-Na in general. The poorer photosensitization effect of DPP-Na when compared to P-Na may be attributed to its lower hydroxyl group density than that of P-Na.

### 3.4. Comparison of IHA-PS (P-Na) with non-polyol type photosensitizers.

In order to further verify the effect of IHA-PS, two non-polyol type photosensitizers – OXT-Na and NDC-OX were synthesized and compared with P-Na for UV curing behavior; the results are shown in Figure 4. Again, it was found that in system ECC-EHMO and ECC-PCL, P-Na has a better photosensitization effect. In system ECC-DOX, though the 120 s conversion for all the coatings are similar, the 3 s conversion of P-Na is still higher than the other coatings, indicating the effectiveness of P-Na in the initial photopolymerization stage. When comparing the results of OXT-Na and NDC-OX with two other polyol type photosensitizers – DPP-Na and PCL-Na – it is noticed that the polyol type photosensitizers generally have a better photosensitization effect than the non-polyol ones; this may be attributed to the IHAP mechanism involving polyol type photosensitizers. Furthermore, by examining the results obtained from all the photosensitizers examined so far, an additional piece of evidence that supports the IHAP mechanism may be noted: In system ECC-EHMO and ECC-PCL, although there exists a large amount of abstractable external hydrogen donors provided by the hydroxyl groups on EHMO and PCL molecules, the typical IHA-PS – P-Na, still exhibited a better photosensitization effect. This again corroborates the proposed IHAP (intramolecular hydrogen abstraction photosensitization) mechanism.

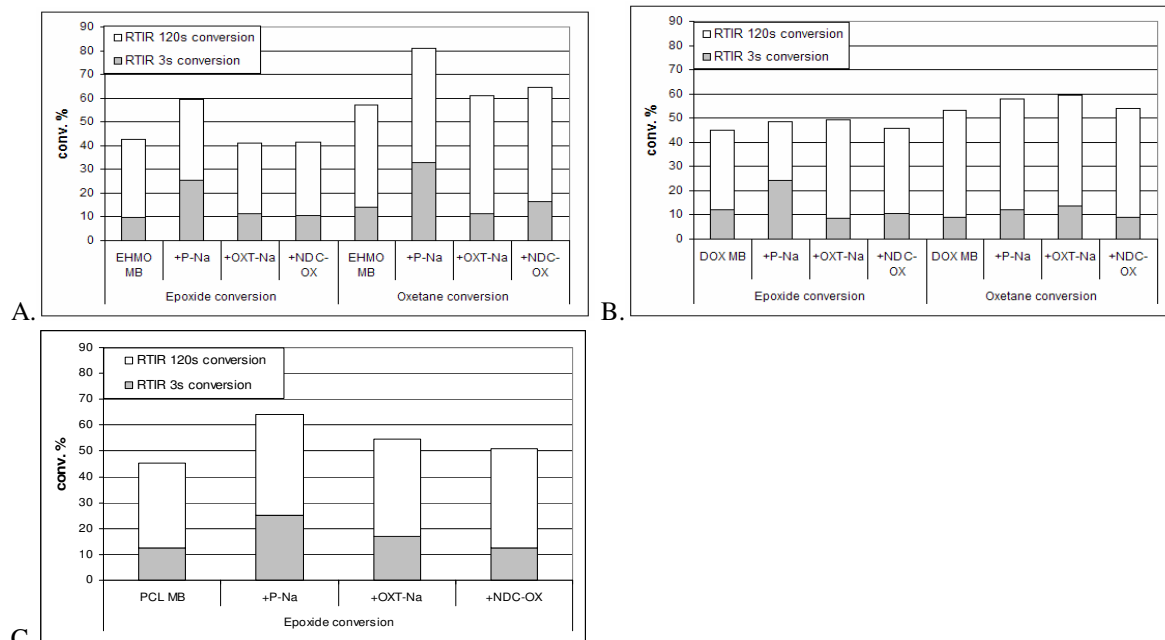


Figure 4. Comparison of functional group conversion for coatings sensitized by P-Na and two non polyol type sensitizers in RTIR experiments. A) System ECC-EHMO, B) System ECC-DOX, C) System ECC-PCL.

### 3.5. The “designed” IHA-PS and its photosensitization effect.

From the discussion on the relationship between polyol based photosensitizers and their corresponding photosensitization effect, it is realized that two principles appear to be indispensable in order for effective intramolecular hydrogen abstraction to occur. The first is the amount of internal abstractable hydrogens sources (hydroxyl groups in this case) around the chromophore (naphthalene in this case). The more the internal hydroxyls, the higher the chance for the ion pair  $\text{Na}^+\text{MtX}_n^-$  to interact and abstract a hydrogen intramolecularly. The second and the most important principle is the relative spatial position of the ion pair and the internal hydroxyls. These hydroxyls must be in a position (as in the case of P-Na) or can move to a position (through chain movement as in the case of DPP-Na) where the collision of the ion pair with the hydroxyl can occur, which is most likely followed by hydrogen abstraction and super acid generation. These two principles can be used in order to design and synthesize a more simplified version of IHA-PS than P-Na. Since on the one hand, the P-Na seems too “clumsy” with a MW of 1650, also it was suspected that only the hydroxyl groups on the same hemisphere as the  $\text{Na}^+\text{MtX}_n^-$  function as an effective abstractable hydrogen source; the other hydroxyl groups on the opposite side of the molecule are redundant. Consequently, we speculated that it is possible for a molecule to exhibit the same photosensitization effect as P-Na with much fewer internal hydroxyls as long as there are sufficient internal hydroxyls around the  $\text{Na}^+\text{MtX}_n^-$ . Additionally, if a simplified version of an IHA-PS molecule having an equal photosensitization effect to P-Na can be designed and synthesized by applying the two proposed principles, it would be a further validation of the proposed IHAP mechanism. So the objective of this simplified IHA-PS project was to synthesize a photosensitizer molecule that exhibits effective IHAP with the least amount of internal hydroxyl groups and lowest molecular weight.

The first step of this molecule design and synthesis project was to determine the topology of the photosensitizer molecule. After consideration of possible molecule topologies such as linear, comb, and even crown ether like topology etc., as well as synthesis feasibility and simplicity, it was decided that an

effective topology would be a hyperbranched structure with the polynuclear aromatic compound semi-buried in the branches functionalized with hydroxyl groups. This way the chromophore still has a chance to interact with the photoinitiator molecule, and, at the same time, the generated super acid species also has a chance to escape from the IHA-PS molecule to initiate polymerization. More importantly, this topology should provide a better chance for the ion pair  $\text{Na}^+\text{MtX}_n^-$  to interact and abstract a hydrogen from the surrounding hydroxyl groups. A feasible synthesis route for molecule having this topology is a divergent synthesis scheme. Thus, the synthetic strategy begins with a multifunctional core with a low MW, followed by the attachment of the polynuclear aromatic compound to one of the functional arms of the core, then the other hydroxyl functionalized arms around the polynuclear aromatic compound are “grown” through the reaction of the remaining functional arms. Because of the convenience and high yield of hydroxyl-acid chloride reaction, it was again chosen as a method to react the polynuclear aromatic compound onto the core; consequently polyols are the best choice for the multifunctional core. It was thought that the most ideal polyol core is pentaerythritol or di-pentaerythritol due to their branched topology and low hydroxyl equivalent weight. But it was found in our initial trial that these two solid polyols were difficult to handle in practice because of their poor solubility and high melting point. An ethoxylated version of pentaerythritol, polyol PP, was then chosen as an alternative. As the result of ethoxylation, the polyol PP is a low viscosity liquid at room temperature, but with a higher hydroxyl equivalent weight than pentaerythritol. PP-Na was successfully obtained by attaching 1-naphthol chloride to PP (see Table 3). The next challenge was how to attach hydroxyl groups around the attached naphthalene starting from PP-Na. One way was to react a highly functional polyol molecule with the remaining hydroxyl groups of PP-Na. It was also estimated that the backbone length of the polyol molecule should be around 5 atoms, and the primary hydroxyl groups should be attached to atom 3 or 4 so that the hydroxyls can semi-surround the naphthalene and have a higher chance to collide and interact with it. This consideration is illustrated in Figure 5 by the nominal structure of the “designed” IHA-PS.

On the other hand, a key factor for the attachment reaction is the functional group the polyol molecule should have in order to react with the hydroxyl groups of PP-Na. It was thought that the ideal polyol molecule should have an oxygen containing heteroatom ring which is linked to multiple hydroxyl groups, so the attachment of “brush” polyol molecule to PP-Na can be accomplished through a ring opening reaction via the hydroxyl groups of PP-Na. An added advantage of a ring opening reaction is that an additional hydroxyl group will be generated. Based on the above thoughts three molecules, glycidol, EHMO and 3,3-(bis)-hydroxymethyloxetane (BHMO), were selected as possible candidates. Their theoretical ring opened products by reaction with the hydroxyl group are shown in Figure 6 from where it can be seen that after ring opening, all of these molecules will generate at least one hydroxyl group at atom 3. For glycidol, one of the two hydroxyls in the product is the less reactive secondary hydroxyl on atom 2. As to EHMO, two primary hydroxyls will be generated on atom 3. Moreover, the EHMO has low viscosity and is readily available. For BHMO, it is the best candidate since 3 primary hydroxyls will be generated on atom 3, but it is not readily available from either commercial sources or through lab preparation.<sup>16</sup> Also, it is not easy to handle due to its solid form and strong hydrogen bonding. So, finally, EHMO was selected for a trial synthesis. The synthesis and characterization of the simplified IHA-PS is described in section 2.2 and 3.1 respectively, its nominal structure is shown in Figure 5, and the product was named PP-Na-ol.

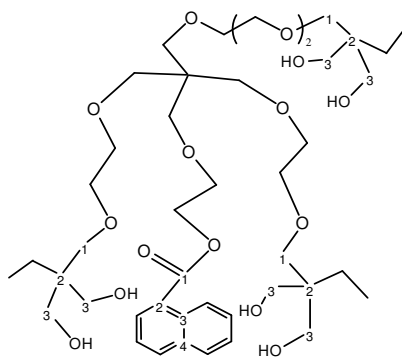


Figure 5. Nominal structure of “designed” IHA-PS – PP-Na-ol.

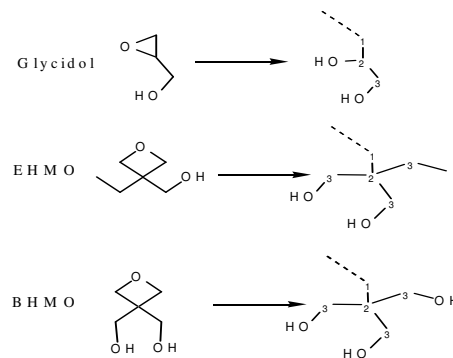


Figure 6. Theoretical ring open products of glycidol, EHMO and BHMO.

The PP-Na-ol and PP-Na were added into aforementioned three formulation systems to make sensitized coatings. The UV curing behavior of these coatings was then monitored by RTIR, and was compared with the blank formulation and P-Na, the results are shown in Figure 7. From Figure 7 it can be seen that the “designed” IHA-PS – PP-Na-ol, exhibits a similar photosensitization effect to P-Na in all of the formulation systems, and excels other photosensitizers studied in this work. More importantly, it should be noticed that the theoretical molecular weight of PP-Na-ol (858) is only half that of P-Na (1655), and its theoretical number of hydroxyls is only one third of P-Na (5 vs. 15). As a result, the PP-Na-ol has much higher hydroxyl equivalent weight (172g/mole) than P-Na (110g/mole). So it can be concluded that by utilizing the proposed principles in the IHAP mechanism, a more simplified version of IHA-PS was synthesized by placing enough internal hydrogen donors in the right relative spatial position to the polynuclear aromatic chromophore. This “designed” IHA-PS has a more efficient IHAP effect in terms of the hydroxyl equivalent weight and molecular weight of the photosensitizer. This result further confirms the proposed IHAP mechanism.

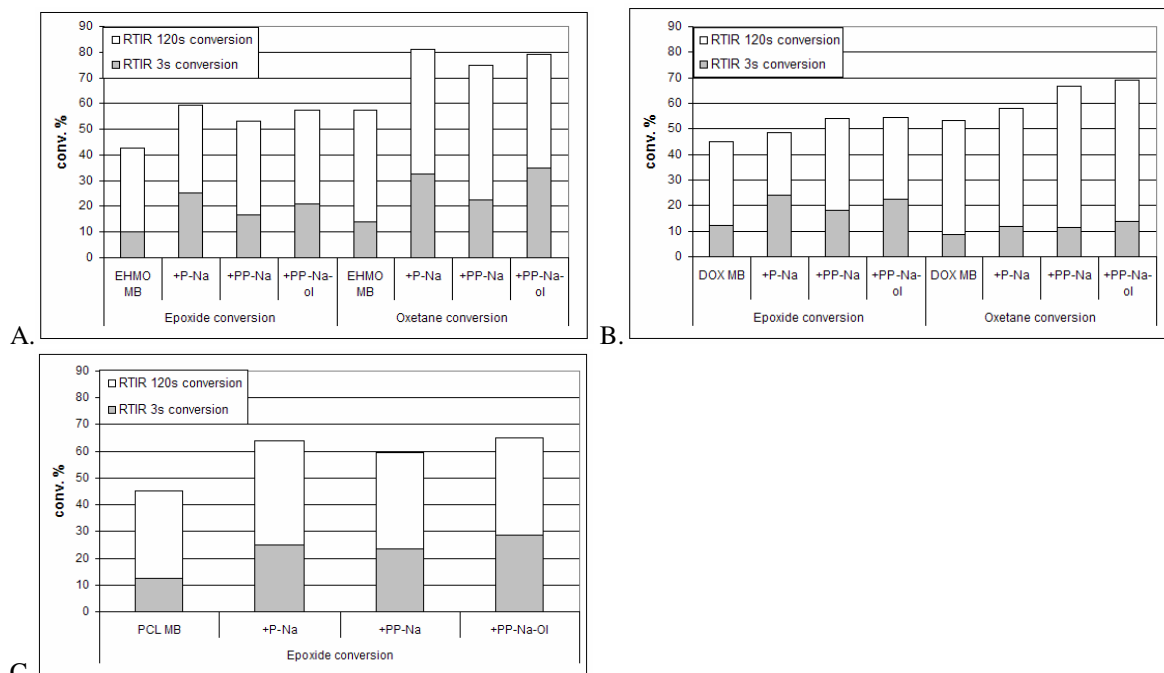


Figure 7. Functional group conversion for coatings sensitized by P-Na, PP-Na and “designed” IHA-PS – PP-Na-ol in RTIR experiments. A) in system ECC-EHMO. B) in system ECC-DOX. C) in system ECC-PCL.

## 4. Conclusions

A series of cationic photosensitizers were synthesized and characterized by HPLC and GC-MS. A particular polyol type photosensitizer – P-Na – was found to have a pronounced photosensitization effect in three different cationic UV curable formulation systems as revealed by RTIR. An *Intramolecular Hydrogen Abstraction Photosensitization* (IHAP) mechanism was proposed to account for this phenomenon. It was also proposed that the key factor for the IHAP mechanism to occur is that a sufficient number of intramolecular hydrogen donors must exist in the right relative spatial positions to the polynuclear aromatic chromophore. A new IHA-PS – PP-Na-ol – was designed and synthesized utilizing the proposed IHAP principles. Though having a much higher hydroxyl equivalent weight and lower molecular weight than P-Na, the PP-Na-ol exhibited similar photosensitization effect to P-Na, which further validates our proposed IHAP mechanism.

## Acknowledgement

The authors thank the Center for Nanoscale Science and Engineering (CNSE) and the Defense Microelectronics Activity (DMEA) for support of this research under grant (DMEA 90-03-2-0303). We also thank David Christianson and Shane Staflien of CNSE for assistance with the GC-MS and HPLC experimentations.

## References

- (1) Lazauskaite, R.; Grazulevicius, J. V. *Environmental and Chemical Physics* **2002**, *24*, 98-117.
- (2) Sangermano, M.; Malucelli, G.; Bongiovanni, R.; Gopzzelino, G.; Peditt, F.; Priola, A. *J. Mater. Sci* **2002**, *37*, 4753-4757.
- (3) Crivello, J.V.; Mao, Z. *Chem. Mater.* **1997**, 1562-1569.
- (4) Crivello, J. V. *Ann. Rev. Mater. Sci.* **1983**, 173-190.
- (5) Crivello, J.V.; Myoungsouk, J. *Journal of Photochemistry and Photobiology A: Chemistry* **2003**, 173-188.
- (6) Crivello, J.V.; Sangermano, M. *Journal of Polymer Science: Part A: Polymer Chemistry* **2001**, *39*, 343-356.
- (7) Gomurashvili, Z.; Crivello, J. V. *Journal of Polymer Science, Part A: Polymer Chemistry* **2001**, *39*, 1187-1197.
- (8) Sangermano, M.; Crivello, J. V. *ACS Symposium Series* **2003**, 242-252.
- (9) Pappas, S. P.; Gatechair, L. R.; Jilek, J. H. *Journal of Polymer Science, Polymer Chemistry Edition* **1984**, *22*, 77-84.
- (10) Fatmanur, K.; Yusuf, Y. *Macromolecular Rapid Communications* **2002**, *23*, 567-570.
- (11) Crivello, J.V.; Bulut, U. *Journal of Polymer Science: Part A: Polymer Chemistry* **2005**, *43*, 5217-5231.
- (12) Hua, Y.; Jiang, F.; Crivello, J. V. *Chem. Mater.* **2002**, 2369-2377.
- (13) Pappas, S. P.; Gatechair, L. R.; Jilek, J. H. *Advances in Organic Coatings Science and Technology Series* **1982**, 103-107.
- (14) Chen, Z.; Webster, D. C. Study of cationic UV curing and UV laser ablation behavior of coatings sensitized by novel sensitizers, *Polymer*, submitted.
- (15) Moorjani, S. K.; Rangarajan, B.; Scranton, A. B. *ACS Symposium Series* **1997**, *673* (*Photopolymerization: Fundamentals and Applications*), 95-106.
- (16) Chen, Y.; Bednarek, M.; Kubisa, P.; Penczek, S. *Journal of Polymer Science, Part A: Polymer Chemistry* **2002**, *40*, 1991-2002.